frontiers | Frontiers in Earth Science

TYPE Original Research
PUBLISHED 22 April 2024
DOI 10.3389/feart.2024.1365516

OPEN ACCESS

EDITED BY
Hu Li,
Southwest Petroleum University, China

REVIEWED BY
Yumao Pang,
Shandong University of Science and Technology, China
Shun He,
Southwest Petroleum University, China
Hamzeh Ghorbani,
Islamic Azad University, Iran

*CORRESPONDENCE
Yue Zhao,
zhaoyue118000@163.com

RECEIVED 04 January 2024
ACCEPTED 08 April 2024
PUBLISHED 22 April 2024

CITATION
An Z, Zhao Y and Zhang Y (2024), Pore heterogeneity analysis and control mechanisms in Cambrian shale of the Shuijingtuo Formation, Yichang area, China. *Front. Earth Sci.* 12:1365516. doi: 10.3389/feart.2024.1365516

Pore heterogeneity analysis and control mechanisms in Cambrian shale of the Shuijingtuo Formation, Yichang area, China

Zhengzhen An[1], Yue Zhao[1,2]* and Yanfei Zhang[3]

[1]Mining College of Liaoning Technical University, Fuxin, China, [2]College of Innovation and Practice Liaoning Technical University, Fuxin, China, [3]Shenyang Geological Survey Center, China Geological Survey, Shenyang, Liaoning, China

This study focuses on understanding the fractal characteristics and controlling factors of micropore structures within organic-rich shale of the Cambrian Shuijingtuo Formation in the Yichang area of Hubei Province. Mineralogy, petrology, and organogeochemical characteristics were confirmed through comprehensive testing methods, including whole-rock X-ray diffraction and organic geochemical analyses. Additional experiments included low-temperature carbon dioxide adsorption, low-temperature nitrogen adsorption, and high-pressure mercury injection. Fractal dimensions of micropores, mesopores, and macropores were calculated using the V-S, FHH, and MENGER sponge models, respectively. Results indicate that the Cambrian Shuijingtuo Formation represents a typical deposit from an alkaline water body, resulting in high-calcareous shale. Fractal dimensions were as follows: micropores (D1) ranged from 2.1138 to 2.3475 (average 2.2342), mesopores (D2) ranged from 2.5327 to 2.7162 (average 2.6171), and macropores (D3) ranged from 2.7361 to 2.9316 (average 2.82905). Correlations were observed between total organic carbon (TOC) content and Ro with D1 and D2 (positive) and D3 (negative). Shale pore volume and specific surface area exhibited positive correlations with D1 and D2 but negative correlations with D3. High bio-deposited silica positively influenced micropore and mesopore development, while clay mineral compaction and dehydration transformations favored macropore development. Carbonate minerals primarily contributed to regular macropores, with complex correlations involving fractal dimensions D1, D2, and D3. The research results provide theoretical support for analyzing pore fractal characteristics of shallow old Marine shale reservoirs and the prediction and development plan of high-quality reservoirs of the Shuijingtuo Formation in the Yichang area.

KEYWORDS

Yichang area, Shuijingtuo Formation, low-temperature gas adsorption, high-pressure mercury injection, fractal dimension, controlling factor

1 Introduction

As an unconventional reservoir, shale typically exhibits low porosity and permeability (Li, 2023). A large number of nanoscale pores and micro-fractures (faults) develop in shale, interweaving with each other to form a complex fissure-pore network. The occurrence states of gas in shale include the free state, adsorption state, and a small amount in the dissolved state (He et al., 2022a; 2022b). The

proportion of gas content in different states is directly related to the pore structure, an important aspect of shale reservoir evaluation (Li et al., 2019a; Li B. et al., 2019). Gas in micropores and small-aperture mesoporous pores is mostly adsorbed on the inner wall of pores, while gas in large-aperture mesoporous pores and macropores is mostly in the free state (Gao et al., 2020; Zhao et al., 2022). The adsorbed gas content in shale gas is about 80% (Liu and Ostadhassan, 2019; Li, 2021), and characterization of pore complexity has become an important aspect of studying shale reservoir performance.

Due to the characteristics of small pore size and strong heterogeneity, the application of conventional reservoir pore characterization methods in shale reservoirs is extremely limited, which brings challenges to the characterization of shale pore structure (Dou et al., 2020). Shale pore types and morphologies can be observed using argon ion-polished scanning electron microscopy (Cheng et al., 2018). High-pressure mercury intrusion and low-temperature gas adsorption methods are employed for pore structure parameter testing. Low-temperature gas adsorption is more precise for micro-to-mesopore characterization (Jiang et al., 2016; Zeng et al., 2021; Abraham et al., 2022; Xia et al., 2022). Due to its larger kinetic diameter, nitrogen analysis introduces greater errors in characterizing micropore structures during low-temperature nitrogen gas adsorption. Carbon dioxide gas, with its smaller kinetic diameter, offers more accurate characterization of micro-pore structures. During high-pressure mercury intrusion experiments, changes occur in the small pore structures under high pressure, making this method mainly suitable for characterizing macropore structures. Scanning electron microscopy and gas adsorption are currently the most commonly used and effective methods for characterizing shale micro-pore structures (Ma et al., 2021).

Shale pore distribution exhibits significant heterogeneity, influenced by the presence and distribution of organic matter and inorganic minerals. This complexity poses challenges in quantitatively assessing shale pore structures. With the application of fractal theory in characterizing pore structures within unconventional reservoirs, numerous scholars have quantitatively characterized the fractal dimension of pores using different theoretical models (Fan et al., 2020a; Zhang et al., 2020). Zhang et al. (2020) calculated the fractal dimension of pores in different small layers in the Weiyuan area using the FHH model and obtained the most favorable reservoir development section at the bottom of small layer 1. Zhao et al. (2022) quantitatively characterized the shale surface's fractal and structural dimensions by conducting low-temperature nitrogen adsorption experiments. Their findings suggest that the content of organic matter and quartz is the main reason for the complexity of the pore structure. Sun et al. (2021) used low-temperature nitrogen adsorption and high-pressure mercury injection experiments to compare and analyze the complexity of shale pores in Qianjiang Sag and pointed out that the existence of oil film would reduce the complexity of pores, while the development of salt minerals would reduce the connectivity of pores. Xie et al. (2022) pointed out in their study of multi-scale fractal characteristics of shale pores using different gas adsorption experiments and high-pressure mercury intrusion experiments that different experimental methods have specific pore size adaptation ranges in characterizing pore complexity. Finding suitable gases as adsorption media and combining high-pressure mercury intrusion experiments can better characterize the complexity of pore sizes at different scales.

Therefore, understanding the pore structure heterogeneity and its controlling factors in shale formations is crucial for predicting and optimizing hydrocarbon production. This study delves into the intricate pore structure of shale formations, focusing specifically on the Longmaxi Formation in Western Hubei, China. We recognized the importance of shale petrology and geochemical characteristics in determining reservoir behavior, so we conducted a series of advanced laboratory experiments. These included low-temperature carbon dioxide and nitrogen adsorption and high-pressure mercury intrusion experiments. These methods allowed us to meticulously quantify the fractal dimensions of micro, meso, and macropores, providing insights into the hierarchical pore structure of the Longmaxi Formation.

Furthermore, we conducted a correlation analysis to elucidate the interplay between major mineral content, pore structure parameters, and fractal dimensions. By exploring their impact on pore complexity, we aim to unravel the underlying mechanisms shaping the heterogeneity of shale pore networks. This research aims to provide valuable theoretical support for upcoming shale oil and gas exploration endeavors, particularly in the Shuijingtuo Formation.

2 Geological setting

Regarding regional geological characteristics, the Huangling area is located in the northern part of the Yangtze Plate, within the complex tectonic zone known as the folded fault belt of Western Hunan and Hubei (Zhang et al., 2019). It lies in the southwestern sector of the Yichang Slope, bounded by the Huangling Anticline to the north and the Yichang Slope to the east (Figure 1A). To the southwest, it interfaces with the Yidu-Hefeng Anticline through the Jiunianxi Fault and Tianyangping Fault (Xu et al., 2022). The region's surface geological environment is complex, featuring numerous thrust faults and well-exposed stratigraphic sequences spanning the Precambrian to the Cenozoic. The Shuijingtuo Formation was deposited within the stable Yangtze Craton basin during the Jinning period. It was confined by the peripheral ancient landmass and shaped by marine transgressions, resulting in a restricted aquatic environment characterized by deep-water continental shelf facies, shallow-water mixed continental shelf facies, and submarine uplifts. Based on lithological and depositional environment differences, the Shuijingtuo Formation can be divided into three members from bottom to top. The lower part of the Shuijingtuo Formation (1st Member) predominantly comprises mudstone and limestone. The middle part of the Shuijingtuo Formation (2nd Member) consists mainly of black organic-rich shale deposited in a deep-water continental shelf environment (Luo et al., 2019a). This interval hosts abundant fossils such as graptolites and benthic algae and serves as the primary gas-bearing interval within the Shuijingtuo Formation. It is laterally parallel but unconformably overlies the underlying Baiyun Limestone Member of the Yimajiahe Formation (Figure 1B). The uppermost segment, the 3rd Member of the Yimajiahe Formation, represents the sedimentary product of a shallow-water mixed continental shelf environment, primarily composed of

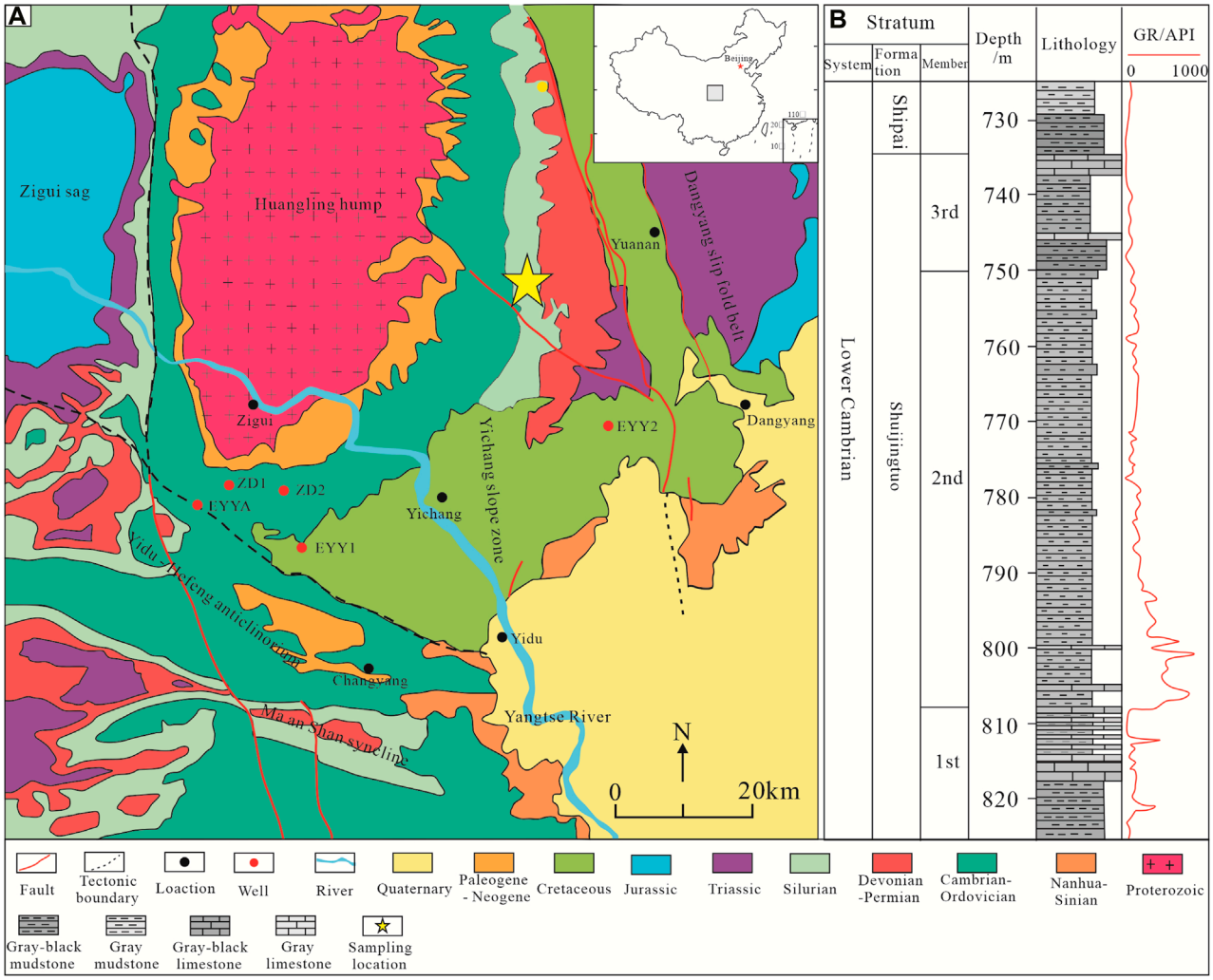

FIGURE 1
Regional structure position **(A)** and comprehensive stratigraphic column chart **(B)** in the study area.

interbedded limestone and clastic rocks. It is conformably overlain by the deep gray mudstone and siltstone of the Shipai Formation (Luo et al., 2019b).

The mudstone shale of the Shuijingtuo Formation has an early formation time and is characterized by a wide lateral distribution, substantial vertical effective thickness, high TOC content, and a high degree of thermal evolution (Zhang et al., 2023). The vertical distribution of TOC content gradually decreases based on typical well analyses. Continuous thicknesses with TOC content greater than 2% extend over 35 m from the base to the top, and thicknesses with TOC content greater than 1% extend over 65 m. The organic matter comprises Type I kerogen, with a minor presence of Type II_1 kerogen. In contrast to the Shuijingtuo Formation shale in the Chongqing and Guizhou regions, it is classified as high-calcium shale, with illite being the predominant clay mineral. The formation is generally buried at depths exceeding 2,000 m, classifying it as mid-shallow shale. Exploration practices have revealed significant variations in gas content and well productivity among different individual wells.

3 Samples and methods

The shale samples analyzed in this study were sourced from outcrop sections around the Huangling Uplift. Before sampling, surface vegetation was cleared, and the upper weathered or weakly weathered layers were removed from the shale outcrops using an excavator. We selected intact and fresh large blocks of shale samples during the sampling process, which were sealed in bags to preserve their integrity. The samples primarily consisted of unweathered, black, organic-rich shale.

3.1 Total organic carbon (TOC) content and maturity testing

We utilized an infrared carbon-sulfur analyzer (LECO CS844) manufactured by the American company LECO to determine the organic carbon content in the black shale samples from the Shuijingtuo Formation. Before experimental testing, fresh black

shale samples were ground in agate mortars until they reached a particle size finer than 80 mesh. The powdered samples were then acid-washed using excess dilute hydrochloric acid for approximately 3 h. After acid washing, the powdered samples were rinsed with distilled water until they reached a neutral PH. Subsequently, the neutral powdered samples were dried at 65°C. The entire testing procedure followed the GB/T 19145-2003 standard, and solid-state infrared absorption was employed to measure the organic carbon content.

We conducted maturity testing using a polarizing microscope (Leica DM4500P) and a microphotometer (CRAIC QDI 302) manufactured by Leica and CRAIC, respectively. Before the experiments, the samples were mechanically crushed and polished. Subsequently, the polished samples were subjected to low-temperature drying at 45°C for 3.5 h in an oven. The experimental procedures followed GB/T 6948-1998 standards and SY/T 5124-2010.

3.2 Whole-rock X-ray diffraction (XRD) analysis

We conducted mineral composition and content analysis of shale using a multifunctional X-ray diffractometer, the Bruker D8ADVANCE, manufactured by Bruker in Germany. The X-ray source employed in the instrument was Cu-target. Before experimentation, shale samples were subjected to low-temperature drying and then finely ground to a particle size exceeding 200 mesh using an agate mortar, ensuring that the sample weight exceeded 0.5 g. The entire testing procedure was conducted at room temperature. During the experiments, the instrument was set to a voltage and current of 40 kV and 5 mA, respectively, and continuous scanning was performed at a minimum diffraction angle of 2°, following the SY/T5163-2010 standard.

3.3 Low-temperature gas adsorption

We conducted low-temperature nitrogen adsorption experiments using an ASAP2420 fully automated surface area and pore size distribution analyzer manufactured by Micromeritics Instrument, United States. Before the experiments, the samples underwent degassing to remove surface impurities. The samples were dried at low temperatures and then ground to a particle size of approximately 40 mesh using an agate mortar. Subsequently, the finely ground powder samples underwent 14 h of vacuum drying at 120°C, with the vacuum pressure below 1 Pa. High-purity liquid nitrogen with a purity exceeding 99.9% was used as the adsorption medium. Under constant temperature conditions at 77 K using liquid nitrogen, the sample's specific surface area, pore size, and pore volume were calculated using the BJH and BET principles (Wang et al., 2018).

We used a pore analyzer produced by Quantachrome Instruments with the model Quadrasorb SI for low-temperature carbon dioxide adsorption experiments. Before testing, the samples were subjected to vacuum treatment at 65°C to eliminate surface moisture. After drying, the samples were placed in liquid carbon dioxide for experimentation.

3.4 High-pressure mercury injection experiment

In this study, we utilized the AutoPore 9510, an automated mercury porosimeter manufactured by Micromeritics Instrument Corporation in the United States. During the testing phase, this instrument allowed for mercury injection pressures of up to 414 MPa, corresponding to a lower limit of approximately 3 nm in test pore size. Before the tests, we shaped the samples into cubes measuring 1 cm × 1 cm × 1 cm.

To minimize the influence of surface roughness on the mercury injection experiment, we employed the instrument to segment the samples, ensuring a flat surface. Before testing, the cubic samples underwent a 60°C drying process lasting 48 h. This step was crucial for eliminating internal impurities and guaranteeing that the original pore structure of the samples remained intact throughout the drying process.

The instrument's internal vacuum was maintained throughout the testing procedure, and the instrument automatically recorded data for mercury intrusion and extrusion processes (Zhu et al., 2019; Zuo et al., 2019).

3.5 Calculation of fractal dimension

The calculation of fractal dimensions involves various models, and the suitability and accuracy of different models vary depending on the pore sizes in question. The calculation methods for fractal dimensions of pores within different size ranges also differ (An et al., 2023). This study employed different calculation models for the fractal dimensions of micropores, mesopores, and macropores to accurately characterize.

In the low-temperature gas adsorption experiment, the kinetic diameter of CO_2 is 0.33 nm, which can be used to characterize the micropores of 0.33–1.4 nm (Shi et al., 2023). The low-temperature carbon dioxide adsorption experiment is well-suited for characterizing micropore complexity (Zhao et al., 2015). The micropore fractal dimension was calculated using the V-S model, with the specific calculation formula presented as follows:

$$LnV1 = \frac{3}{D1}\mathrm{Ln}S + \mathrm{k} \tag{1}$$

In the equation: "k" represents a dimensionless constant; "V_1" denotes the cumulative pore volume, measured in mL/g; "S" stands for the cumulative specific surface area, measured in m^2/g; "D1" represents the micropore fractal dimension, which is dimensionless.

Due to the activation and diffusion effect of nitrogen in micropores and the capillary condensation phenomenon in macropores, the application effect in mesoporous pores is better, so Low-temperature nitrogen adsorption experiments are well-suited for characterizing mesopores (Liu et al., 2023). The fractal dimension of mesopores in shale, as calculated using the FHH model, is determined by the following specific formula:

$$LnV = \mathrm{k} + (D2 - 3)Ln\left[Ln\left(P_0/P\right)\right] \tag{2}$$

In the equation: "k" is a dimensionless constant; "V" represents the cumulative pore volume of a specific stage (e.g., mesopores), measured in mL/g; "P_0" is the vapor pressure of the gas at saturation,

measured in MPa; "*P*" stands for the system's equilibrium pressure, measured in MPa; "D2" is the fractal dimension of mesopores and is dimensionless.

In the process of using high-pressure mercury injection to characterize pore structure, excessive pressure will destroy shale pores, affecting the experimental results, and it is suitable for macro pore characterization (>50 nm) (Wang et al., 2015). Therefore, High-pressure mercury injection experiments have a natural advantage in characterizing shale macropores (Kong et al., 2020). The fractal dimension of macropore porosity is calculated using the MENGER sponge model, with the specific formula provided as follows:

$$D3 = 4 + Ln\left(\mathrm{d}V_{\mathrm{p}}/d_p\right)/LnP \tag{3}$$

Where: "D3" is the macropore fractal dimension (dimensionless); "V_p" is the incremental pore volume (mL/g); "*P*" is the experimental pressure (MPa).

4 Results

4.1 Organic geochemical and petrological characteristics

The results of organic matter content and maturity testing show significant variations in the organic matter content of the Shuijingtuo Formation shale in the Yichang area. The overall content ranges from 0.88% to 4.62%, with an average of 2.56%. The equivalent vitrinite reflectance (Ro) values of organic matter range from 2.05% to 2.74%, with an average of 2.41%.

The whole-rock X-ray diffraction results reveal the complex mineral composition of the Shuijingtuo Formation shale (Table 1). The primary mineral types include feldspar, quartz, calcite, dolomite, and clay, among other major rock-forming minerals. Additionally, pyrite and siderite are notable occurrences. Among these, siliceous and clay minerals are the predominant rock-forming minerals, constituting over 70% of the total mineral content. Quartz content varies between 46% and 64%, with an average of 55.33%, while feldspar content ranges from 3% to 11%, averaging 6%. Clay mineral content falls between 14% and 35%, averaging 23.92%. Carbonate minerals account for 7%–19% of the composition, averaging 11.17%. Calcite content varies from 3% to 14%, averaging 6.8%, while dolomite content ranges from 2% to 7%, averaging 4.3%. Pyrite content is between 1% and 5%, with an average of 2.75%.

4.2 Shale porosity characteristics

Based on DFT, BJH models, and Washburn equations, low-temperature CO_2, N_2 adsorption data, and high-pressure mercury experiment data are processed to obtain the pore volume and specific surface area of micropores, mesoporous, and macropores. The experimental results revealed a total pore volume ranging from 12.63×10^{-3} to 28.71×10^{-3} mL/g, with an average pore volume of 19.50×10^{-3} mL/g (Table 2). Among these values, micropore volume varied between 1.56×10^{-3} and 7.64×10^{-3} mL/g, averaging at 4.228×10^{-3} mL/g, constituting an average of 21.26% of the total. Mesopore volume ranged from 3.77×10^{-3} to 15.58×10^{-3} mL/g, averaging at 7.925×10^{-3} mL/g, representing an average of 39.76%. Macropore volume fell between 4.85×10^{-3} and 11.4×10^{-3} mL/g, with an average of 7.35×10^{-3} mL/g, making up 38.98% of the total.

The shale's total specific surface area spanned from 9.54 to 17.54 m^2/g, with an average specific surface area of 13.55 m^2/g. Within this range, micropore specific surface area fluctuated between 6.84 and 13.42 m^2/g, averaging at 9.91 m^2/g, representing an average of 72.52%. Mesopore specific surface area ranged from 2.52 to 4.14 m^2/g, averaging at 3.19 m^2/g, averaging 24.11%. Macropore specific surface area ranged from 0.18 to 0.84 m^2/g, with an average specific surface area of 0.45 m^2/g, constituting an average of 3.35%.

4.3 Fractal dimension characteristics of pore structure

We determined the micropore fractal dimension, calculated using the V-S model, as D1; we denoted the mesopore fractal dimension, calculated using Eq. (1) the FHH model, as D2; and we assigned the macropore fractal dimension, calculated using Eq. (2) the MENGER sponge model, as D3 Eq. (3). According to the results obtained from these different models, there are significant variations in the micropore, mesopore, and macropore fractal dimensions. Specifically, D1 values for the samples range from 2.1138 to 2.3475, with an average of 2.2342. D2 values range from 2.5327 to 2.7162, with an average of 2.6171. D3 values range from 2.7361 to 2.9316, with an average of 2.82905 (Table 3).

The fractal dimension of pore structures in shale samples falls within the range of 2–3. A higher fractal value indicates a more complex pore system within the shale. The calculation results reveal a clear relationship of D1 < D2 < D3 (Figure 2). Notably, D1 is relatively close to the lower limit of the fractal theory, suggesting that micro-pores in the Shuijingtuo Formation shale have smoother surfaces and lower roughness, indicating a relatively simple pore structure. On the other hand, the maximum fractal dimension of macropores exceeds 2.9, approaching the theoretical upper limit, indicating that macropore structures in the Shuijingtuo samples are more complex with rougher pore surfaces.

5 Discussion

5.1 Shale pore heterogeneity influencing factors

The strong heterogeneity of pores in shale directly affects the gas occurrence state and flow mode. Pore heterogeneity is influenced by multiple factors, among which diagenetic minerals and organic matter are the two decisive factors affecting pore development (Li et al., 2019c; Fan et al., 2020b). Organic matter pyrolysis determines the morphology and development degree of organic pores (Borjigin et al., 2021), while diagenetic minerals affect the type and distribution of inorganic pores (Hao et al., 2022; Yin et al., 2022). Therefore, this study mainly explores

TABLE 1 Organic geochemistry and mineral composition characteristics of shale samples.

Sample number	TOC (%)	Ro (%)	Quartz (%)	Feldspar (%)	Calcite (%)	Dolomite (%)	Pyrite (%)	Sphalerite (%)	Clay minerals (%)
SJT-1	3.61	2.05	52	2	11	8	1	1	25
SJT-2	4.27	2.74	63	10	4	3	4	2	14
SJT-3	2.35	2.33	55	4	14	3	3	0	21
SJT-4	1.72	2.42	61	9	3	5	2	0	20
SJT-5	0.88	2.13	46	11	3	4	1	0	35
SJT-6	2.64	2.53	59	8	11	2	3	1	16
SJT-7	1.27	2.42	49	7	4	6	2	1	31
SJT-8	1.09	2.21	47	10	5	3	4	2	29
SJT-9	1.82	2.34	51	6	10	8	2	1	22
SJT-10	2.83	2.55	52	5	7	7	3	1	25
SJT-11	3.66	2.64	52	2	3	4	3	2	34
SJT-12	4.62	2.55	64	3	4	6	5	1	17

TABLE 2 Pore structure parameters of shale samples.

Sample number	Pore volume ($\times10^{-3}$ mL/g)				Specific surface area (m^2/g)			
	Total	Micropore	Mesopore	Macropore	Total	Micropore	Mesopore	Macropore
SJT-1	20.37	4.24	7.53	8.6	12.45	8.12	4.14	0.19
SJT-2	28.71	7.64	15.58	5.49	15.87	11.86	3.57	0.44
SJT-3	20.92	5.09	8.03	7.8	16.08	12.55	3.06	0.47
SJT-4	21.46	3.42	9.47	8.57	12.63	9.54	2.88	0.21
SJT-5	12.63	1.56	3.77	7.3	9.54	6.84	2.52	0.18
SJT-6	19.27	4.43	8.52	6.32	13.57	10.34	3.02	0.21
SJT-7	17.59	3.68	5.73	8.18	12.04	8.84	2.84	0.36
SJT-8	13.42	2.25	5.16	6.01	11.53	7.54	3.15	0.84
SJT-9	18.35	5.25	7.01	6.09	11.72	7.57	3.53	0.62
SJT-10	20.54	4.18	8.78	7.58	13.44	9.03	3.51	0.9
SJT-11	22.53	3.58	7.55	11.4	16.21	13.42	2.55	0.24
SJT-12	18.19	5.37	7.97	4.85	17.54	13.27	3.54	0.73

the controlling factors of shale pore heterogeneity from the relationship between organic matter content, maturity, inorganic mineral content, pore volume, specific surface area, and different fractal dimensions.

5.1.1 Influence of shale organic geochemical characteristics on heterogeneity

Organic pores are the most important pore type in mature organic-rich shale. The irregular and scattered distribution of

TABLE 3 Distribution table of fractal dimension of shale samples.

Sample number	Micropore fractal dimension (D1)	Mesopore fractal dimension (D2)	Macropore fractal dimension (D3)
SJT-1	2.2328	2.6848	2.7984
SJT-2	2.3059	2.6837	2.8654
SJT-3	2.2108	2.5948	2.8316
SJT-4	2.1852	2.6126	2.9068
SJT-5	2.1138	2.5547	2.9316
SJT-6	2.2758	2.6038	2.7938
SJT-7	2.1347	2.6474	2.8453
SJT-8	2.1909	2.5327	2.9136
SJT-9	2.2743	2.5384	2.7754
SJT-10	2.2039	2.5779	2.8125
SJT-11	2.3343	2.6587	2.7361
SJT-12	2.3475	2.7162	2.7381

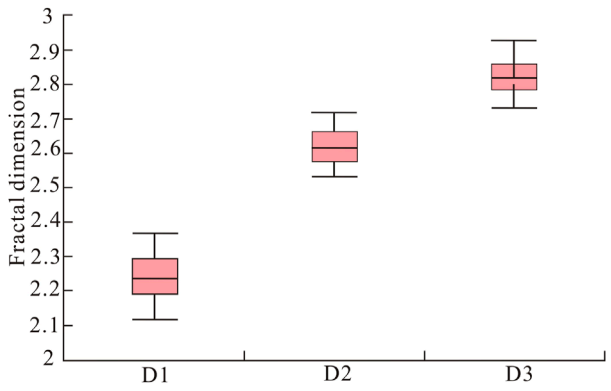

FIGURE 2
Box diagram of fractal dimension of different shale pores in the Shuijingtuo Formation.

organic matter in shale is one of the important reasons for the uneven distribution of organic pores. Organic matter is the basis for developing hydrocarbon-generating pores, and a certain degree of maturity is necessary for the thermal decomposition of organic matter to form pores. The two jointly control the development of organic matter (Cao et al., 2016; Li et al., 2022; Fan et al., 2024).

To further analyze the impact of organic matter content and maturity on pore heterogeneity, we conducted statistical and regression analyses to assess the relationships between organic matter content, maturity, and the fractal dimensions of micro, meso, and macro-pores. The results demonstrated a strong positive correlation between shale organic matter content and D1, with a correlation coefficient of 0.6797. Similarly, a significant positive correlation was observed between organic matter content and D2, with a coefficient of 0.5167. However, there was a moderate negative correlation between organic matter content and D3, with a correlation coefficient of 0.448 (Figure 3A).

The development of hydrocarbon-producing pores is directly linked to the thermal maturity of organic matter. Before reaching the late over-maturity stage, the number of hydrocarbon-producing pores increases with growing maturity, leading to irregular changes in pores of different sizes. According to the correlation analysis between shale sample fractal dimensions and maturity, during the early stages of high-over-maturity, there is a positive correlation between organic matter maturity and both D1 (correlation coefficient of 0.4344) and D2 (correlation coefficient of 0.4851). However, there is an overall decreasing trend in the relationship between maturity and D3, although the correlation coefficients are relatively low (Figure 3B).

Based on the correlation analysis between organic matter content and pore volume, as well as surface area, we found that the correlation coefficients between organic matter content and micro-pore surface area and pore volume were 0.5248 and 0.4939, respectively. For mesopores, the correlation coefficients were 0.2643 for surface area and 0.4113 for pore volume (Figures 3C, D). However, there was no significant correlation between organic matter content and macro-pore volume and surface area. This suggests that organic matter primarily contributes to micro and meso-pores.

During the early stages of over-maturity, organic matter undergoes thermal decomposition and gas generation phases The substantial loss of organic matter reduces its "supporting capacity," leading to the collapse of organic matter (Li et al., 2020; Wu and

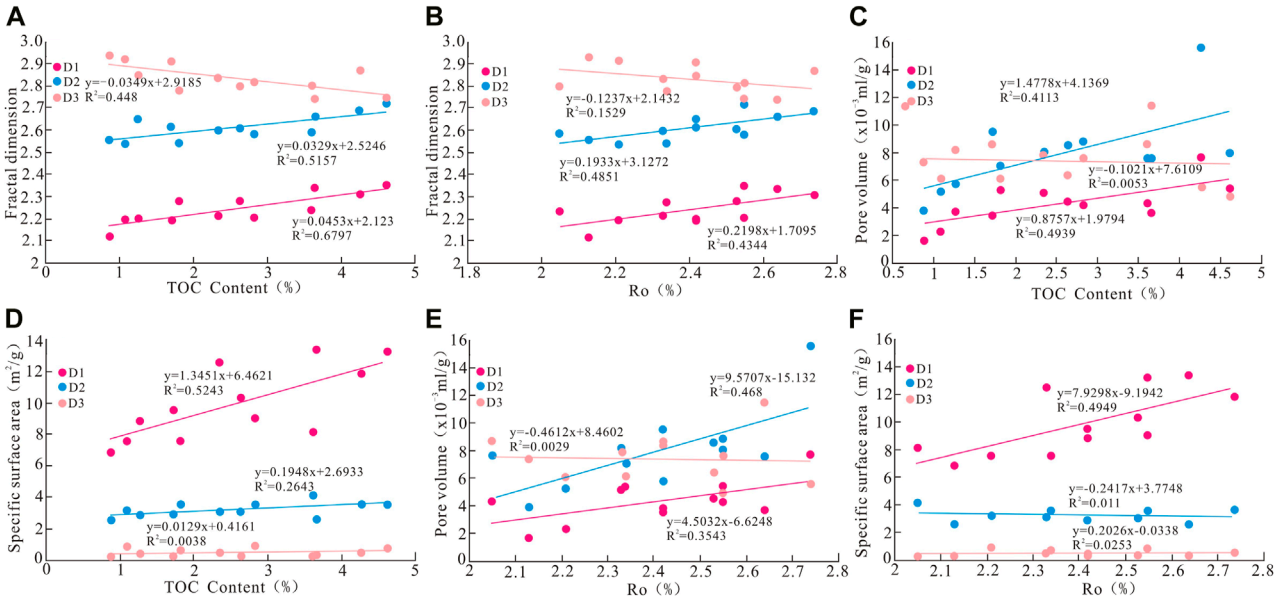

FIGURE 3
The relationship between the basal localization characteristics, the pore structure parameters, and the fractal dimension of shales in the Shuijingtuo Formation. **(A)** Fractal dimension and TOC; **(B)** Fractal dimension and Ro; **(C)** Pore volume and TOC; **(D)** Specific surface area and TOC; **(E)** Pore volume and Ro; **(F)** Specific surface area and Ro.

Lei, 2022). This phenomenon results in the extensive development of pores, and as hydrocarbon generation intensifies, the original pore sizes expand, increasing pore heterogeneity.

As organic matter content increases, various pore sizes receive some degree of stimulation, with the most substantial increase occurring in micro-pores, followed by meso-pores, while macro-pores show the least increase. Combining this with the earlier comparison of micro, meso, and macro-pore fractal dimensions, micro-pores exhibit the smallest fractal dimension, indicating simpler pore structures. With increasing organic matter content, both the quantity and heterogeneity of micro and mesopores increase, leading to higher values of D1 and D2.

As previously discussed, the organic matter in the study area is in a state of high-over maturity. The correlation coefficients between the thermal maturation level of shale samples and the fractal dimensions of micro and mesopores are moderate (Figures 3E, F).

On the one hand, as the thermal maturation level increases, organic matter undergoes more intense hydrocarbon generation, increasing the quantity of micro, meso, and macro-pores. During the over-maturity stage, as the thermal maturation level continues to rise, organic matter undergoes aromatization (Wu and Lei, 2022), which increases the roughness of pore walls and weakens the supporting capacity of pores for overlying strata. This results in irregular deformation of pores and an increase in the irregularity of pore shapes, leading to an increase in the fractal dimensions of micro and mesopores.

Regarding macropores, as the thermal maturation level increases, some mesopores continue to expand into macropores, increasing the total quantity of macro-pores. These macropores are often elliptical or circular, which, to some extent, reduces the fractal dimensions of macropores. This weakening effect on the complexity of macro-pores, along with the contribution of regularly shaped macropores by inorganic minerals, results in a lack of a strong correlation between the fractal dimensions of macropores and thermal maturity in the study area.

5.1.2 Relationship between shale pore structure parameters and fractal dimensions

Pore volume and specific surface area are characteristic parameters for evaluating shale gas storage capacity. The larger the pore volume, the larger the gas storage space; the larger the specific surface area, the stronger the gas adsorption capacity. The fractal dimension can quantify the complexity of pores and affect the ratio of adsorbed gas to free gas in shale. Therefore, a natural inherent relationship exists between pore volume, specific surface area, and fractal dimension.

According to the results of the correlation analysis between sample pore volume, specific surface area, and fractal dimensions, strong positive correlations were observed between micropore-specific surface area and D1, with correlation coefficients of 0.6202 (Figure 4A). In contrast, the correlation between micro-pore volume and D1 was weaker, with a coefficient of 0.3056 (Figure 4B). Mesopore specific surface area exhibited a significant positive correlation with D2, with a coefficient of 0.5946, while the correlation coefficient between mesopore volume and D2 was 0.31. In contrast, macro-pore volume and specific surface area showed an overall negative correlation with D3, but the correlation coefficients were smaller than D1 and D2.

Considering the contribution rates of micro, meso, and macro-pore specific surface areas and volumes, it can be observed that an increase in micro-pore fractal dimension is associated with an increase in pore volume and specific surface area. When pore

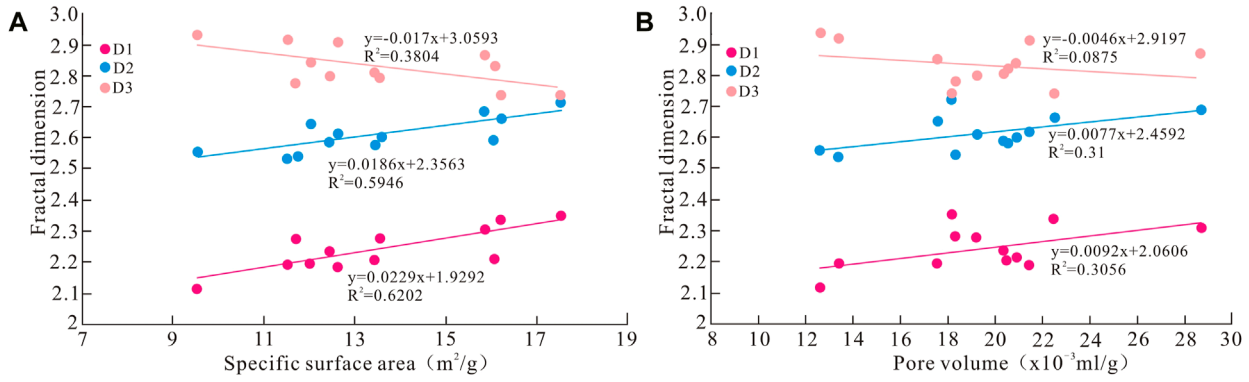

FIGURE 4
Correlation between specific surface area **(A)**, pore volume **(B)**, and fractal dimension of shales in the Shuijingtuo Formation.

volume and specific surface area increase, it indicates an increase in the number of micro-pores in shale, along with an increase in the uneven distribution of these micro-pores and their differences in pore size, leading to an increase in the fractal dimension. As meso-pore sizes increase, the specific surface area provided by mesopores gradually decreases while pore volume increases. According to pore fractal theory, larger mesopore sizes correspond to larger fractal dimensions. The substantial difference in mesopore sizes results in a relatively weak overall correlation with D2. For macro-pores, an increase in specific surface area implies a decrease in the proportion of macro-pores in shale, leading to a certain degree of reduction in fractal dimension.

5.1.3 Impact of mineral composition on pore structure heterogeneity

Shale inorganic minerals can be divided into three categories: siliceous, clay, and carbonate. Different diagenetic minerals have significant differences in their resistance to compaction and dissolution (Huang et al., 2020), resulting in differences in pore types, contents, and pore sizes provided by different minerals during long-term burial diagenesis. The differences in mineral content and uneven distribution among different types of minerals in shale are important factors that increase the complexity of shale pores. In this study, we established correlations between the content of these three mineral categories and structural parameters, including pore volume, specific surface area, and fractal dimensions. The results indicate that the content of siliceous minerals exhibits a positive correlation with the micro- and mesopore volumes in shale, with correlation coefficients of 0.4941 and 0.5796, respectively (Figure 5A). However, it shows a negative correlation with the macropore volume, with a lower correlation coefficient. It exhibits a clear positive correlation with the specific surface area of micro-pores but does not show significant correlations with mesopores or macropores (Figure 5B). Considering the sedimentary environment and the source of siliceous minerals, the Wellsboro Formation was formed in an anoxic deep-water continental shelf (Zhang LL. et al., 2023). The warm water conditions were conducive to the proliferation of siliceous microorganisms, and the siliceous shells were preserved in anoxic water after their death. At the same time, biological soft tissue increased the organic matter content. A substantial portion is derived from organic matter and the correlation between siliceous minerals and organic matter content. Biological skeletons and the accumulation of organic matter typically exhibit significant zonation. According to the correlation curves between siliceous mineral content and the three types of pore fractal dimensions, siliceous minerals show a moderate positive correlation with D1 and D2, with correlation coefficients of 0.3258 and 0.3933, respectively, while exhibiting a weaker negative correlation with D3, with a correlation coefficient of 0.1191 (Figure 5C).

As one of the major diagenetic minerals, clay minerals play a crucial role as carriers for pore development in shale. The types and characteristics of pore development are influenced by the way minerals accumulate and their structure. The “layered stacking” of clay minerals and the “contact-embedded” distribution with other brittle minerals easily lead to numerous intergranular pores. Typically, such pores have irregular shapes and relatively large diameters.

In the case of the Shuijingtuo Formation, which formed early, montmorillonite undergoes dehydration and transformation due to compaction and temperature effects during the sediment compaction process. This increases the pore size within clay minerals as illite and illite-smectite interlayers become more abundant. Analyzing the correlation between clay mineral content and shale pore volume and specific surface area, it is observed that the volumes of micro and macropores and specific surface area in shale decrease as the content of clay minerals increases (Figures 5D, E). This phenomenon is primarily associated with clay minerals’ compaction and diagenetic transformation. There is, however, a certain positive correlation with macropore volume, mainly because clay minerals have larger pore diameters. An increase in clay mineral content significantly increases the number of these macropores, increasing macropore volume.

When comparing clay mineral content with different pore size fractal dimensions, a weak negative correlation is found between clay mineral content and D1 and D2, while a weak positive correlation is observed with D3 (Figure 5F). Although the correlation coefficients are relatively small, in conjunction with the source of macropores, it becomes evident that organic matter, siliceous minerals, and carbonate minerals in shale all contribute to

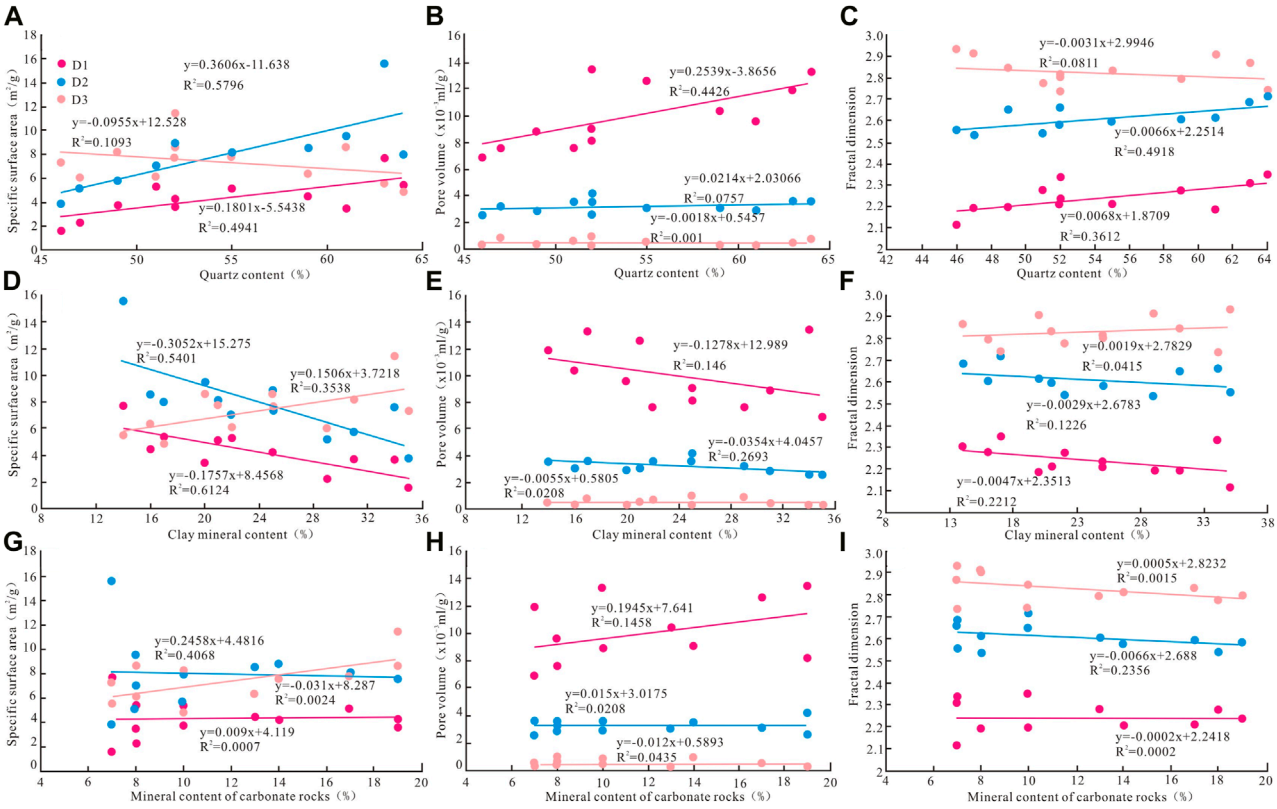

FIGURE 5
Correlation between inorganic minerals and pore structure parameters and fractal dimension. **(A–C)** Quartz content; **(D–F)** Clay mineral content; **(G–I)** Mineral content of carbonate rocks.

a certain amount of macropores. This leads to a less pronounced correlation between clay mineral content and D3. Clay minerals provide a variety of pore types with significant differences in pore size, primarily developing macropores. The varying contributions of clay minerals to the three categories of pore sizes interact with the contributions of other minerals, resulting in the complexity of fractal dimensions in pores of different sizes.

As one of the major diagenetic minerals, the shale in the Shuijingtuo Formation contains two carbonate minerals, calcite, and dolomite, with their content not exceeding 20%. Their distribution in the shale is highly heterogeneous. Being easily soluble minerals, they are prone to dissolution by groundwater under burial conditions, forming dissolution pores. Meanwhile, carbonate minerals located near organic-rich zones are susceptible to dissolution by organic acids produced during the thermal maturation of organic matter, resulting in a limited number of dissolution pores.

Through the analysis of the correlation between the content of carbonate minerals and structural parameters such as micropore, mesopore, and specific surface area in shale, it was found that there was no significant correlation between the content of carbonate minerals and micro-pore or mesopore pore volume or specific surface area. However, a certain positive correlation was observed between the content of carbonate minerals and macro-pore pore volume, with a correlation coefficient of 0.4068 (Figures 5G, H).

Taking into account the correlation between the content of carbonate minerals and the fractal dimensions of pores of different sizes, it was found that there was a weak negative correlation between the content of carbonate minerals and both D1 and D2, while a promoting effect was observed with D3 (Figure 5I). This suggests that carbonate minerals in the shale primarily contribute to macropores' development. The increase in the content of carbonate minerals, combined with their uneven distribution, effectively enhances the complexity and heterogeneity of macro-pore development.

Combined with the correlation between inorganic minerals, TOC, and different pore fractal dimensions, inorganic minerals and TOC content have different control effects on the pore fractal dimension (Figure 6). Siliceous minerals and organic matter promote the complexity of pores, while clay minerals and carbonate minerals have a weak negative correlation or no obvious correlation with the complexity of pores. This phenomenon is related to the pore types and existing forms provided by different minerals. Organic matter in shale shows a diffuse distribution and many irregular pores are formed by stacking organic matter and hydrocarbon pyrolysis. There are obvious differences in pore size, which greatly increases the complexity of pores. While a large amount of organic matter comes from the burial and accumulation of microorganisms, whose siliceous shells and skeletons form biosilicon, and siliceous minerals increase the supporting capacity between minerals. In compaction, the pores can maintain their original state and weaken the "uniformity" of pore morphology caused by compaction. Therefore, organic matter and siliceous minerals contribute the

10.3389/feart.2024.1365516

Variables	Siliceous mineral	Carbonate mineral	Clay minerals	TOC	D1	D2	D3
Siliceous mineral	1						
Carbonate mineral	-0.2186	1					
Clay minerals	-0.6429	0.0224	1				
TOC	0.415	0.1552	-0.257	1			
D1	0.7163	/	-0.2212	0.682	1		
D2	0.512	-0.2356	-0.1226	0.6629	0.4332	1	
D3	-0.5995	/	-0.0415	0.3665	-0.6559	-0.1777	1

FIGURE 6
Influencing factors of shale pore complexity.

most to pore complexity. However, carbonate minerals and clay minerals mainly provide large pore mesoporous and macro pores. According to fractal theory, increasing macro pore will reduce pore complexity.

5.2 Geological significance of fractal dimensions of shale pores

The pore structure of shale determines the occurrence state and flow mode of hydrocarbon molecules within the layer (Tian et al., 2016). The heterogeneity of pores also controls the storage performance of shale and the micro permeability of shale gas. Generally speaking, the more complex the pore structure, the more difficult the gas migration within the layer (Xiong et al., 2017), and the macroscopic manifestation is the decrease in the permeability of the storage mechanism. For different gas contents in different states, the stronger the heterogeneity of pores, the higher the proportion of adsorbed gas content. Therefore, the larger the fractal dimension, the more complex the shale pore structure, the stronger the heterogeneity, and the more unfavorable it is for shale gas development.

Combining the statistical analysis of fractal dimensions for different pore sizes in the Shuijingtuo Formation, it is evident that the fractal dimension for macro-pores is larger, while those for meso and micro-pores are smaller. This suggests that macro-pores exhibit stronger adsorption capabilities. When comparing the contribution rates of pore volume and specific surface area for the three pore categories, micro-meso pores, with smaller diameters, have a higher proportion than macro-pores. Specifically, micro-meso pores account for over 60% on average, with micropores specific surface area making up over 70%. These micro-pores offer more surface adsorption sites, resulting in a greater "adsorption potential" on the pore walls and weaker gas molecule "flowability."

In contrast, macro-pores have larger diameters. Although their rough and complex pore walls enhance gas molecule adsorption, numerous hydrocarbon molecules diffuse freely within these pores. The presence of these hydrocarbon molecules increases the shale's permeability. Consequently, a higher macropore content for shale reservoirs leads to greater matrix permeability.

Regarding gas occurrence within the strata, In terms of the gas occurrence state in the shale, the adsorption gas occupies a large space in the shale micropores (Figure 7A). The gas is mostly in the form of adsorbed gas; the content of adsorbed gas is small, and the gas fluidity is weak. The area occupied by adsorbed gas in the mesoporous pores increases (Figure 7B), and the proportion of adsorbed gas content decreases. With the further increase of the pore size, the proportion of adsorbed gas content in the macropores decreases (Figure 7C), the free gas content increases in the middle of the pores, and the gas fluidity increases.

Larger fractal dimensions for micro and mesopores indicate stronger pore structure and heterogeneity. This results in weaker gas adsorption capabilities, leading to a higher proportion of adsorbed gas content in shale, with over 57% being the maximum observed in the Shuijingtuo Formation. On the other hand, macro-pores,

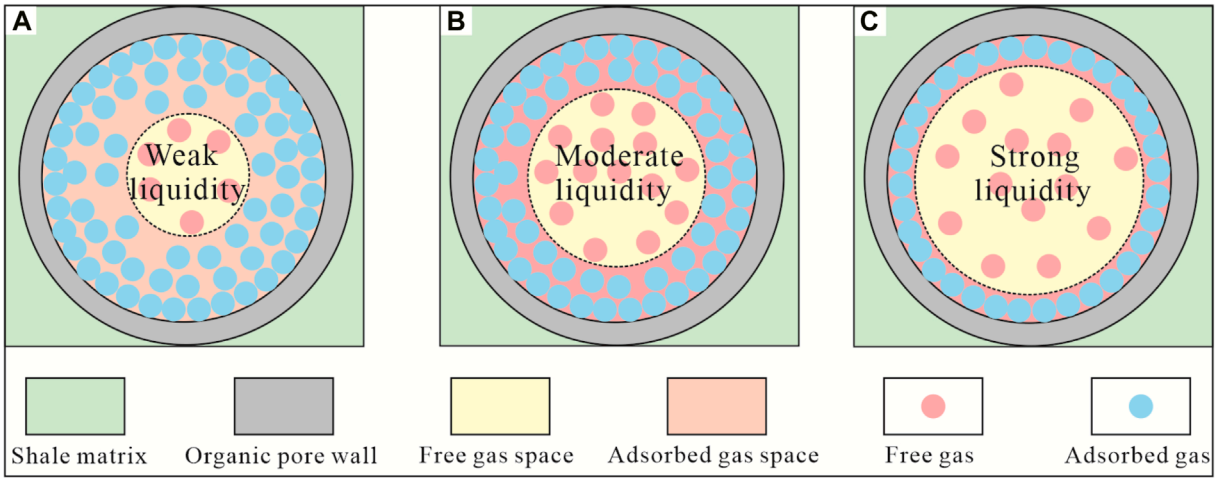

FIGURE 7
Differences in shale gas occurrence with different shale pore sizes. **(A)** Shale micropores; **(B)** Shale mesopores; **(C)** Shale macropores.

with their larger diameters, predominantly host gas molecules in a free state.

6 Conclusion

(1) In the Huangling area, the Shuijingtuo Formation exhibits an organic matter content ranging from 0.88% to 4.26%, with Ro values falling between 2.05% and 2.74%, averaging at 2.409%. This indicates a state of high to over-maturity. The shale comprises approximately 54%–73% silica minerals, averaging 60.67%. Calcium minerals account for 7%–19%, averaging 11.17%, while clay minerals have an average content of 24%. These characteristics point to the formation of calcareous shale in an alkaline aquatic environment.

(2) Utilizing low-temperature nitrogen and carbon dioxide adsorption and high-pressure mercury intrusion experiments, micropore, mesopore, and macropore fractal dimensions were computed using the V-S, FHH, and MENGER Sponge models. The micropore (D1) ranged from 2.1138 to 2.3475, averaging 2.2342. The mesopore (D2) ranged from 2.5327 to 2.7162, averaging 2.6171. The macropore (D3) ranged from 2.7361 to 2.9316, averaging 2.82905.

(3) Organic matter is the foundation for shale micromeso pores, while maturity promotes hydrocarbon generation through organic matter pyrolysis. The combined effect of these factors contributes to the development of the shale's primary micromeso pores, promoting the shale's specific surface area. This relationship is positively correlated with D1 and D2 but negatively correlated with D3. Silica minerals and organic matter development exhibit a synergistic relationship, positively correlating with D1 and D2. Clay minerals primarily contribute to macro-pores in the shale, showing a positive correlation with shale macro-pore volume and a weak positive correlation with D3. In contrast, carbonate rocks mainly contribute to dissolved macropores, displaying a positive correlation with macropore volume but no significant correlation with pore fractal dimensions.

Data availability statement

The original contributions presented in the study are included in the article/Supplementary material, further inquiries can be directed to the corresponding author.

Author contributions

ZA: Conceptualization, Data curation, Formal Analysis, Investigation, Methodology, Software, Writing–original draft, Writing–review and editing. YuZ: Conceptualization, Formal Analysis, Funding acquisition, Project administration, Supervision, Validation, Writing–original draft, Writing–review and editing. YaZ: Formal Analysis, Investigation, Resources, Validation, Writing–original draft.

Funding

The author(s) declare that no financial support was received for the research, authorship, and/or publication of this article.

Conflict of interest

The authors declare that the research was conducted in the absence of any commercial or financial relationships that could be construed as a potential conflict of interest.

Publisher's note

References

Abraham, R. M., Taioli, F., and Nzekwu, A. I. (2022). Physical properties of sandstone reservoirs: implication for fluid mobility. *Energy Geosci.* 3 (4), 349–359. doi:10.1016/j.engeos.2022.06.001

An, C., Liu, G. D., Sun, M. L., You, F. L., Wang, Z. X., and Cao, S. Y. (2023). Analysis of shale pore structure characteristics based on nitrogen adsorption experiment and fractal FHH model: a case study of 7th member of Triassic Yanchang Formation in Huachi area, Ordos Basin. *Petrol. Geol. Exp.* 45 (3), 576–586. doi:10.11781/sysydz202303576

Borjigin, T., Lu, L. F., Yu, L. J., Zhang, W. T., Pan, A. Y., Shen, B. J., et al. (2021). Formation, preservation and connectivity control of organic pores in shale. *Petrol. explor. Dev.* 48 (4), 798–812. doi:10.1016/S1876-3804(21)60067-8

Cao, T. T., Song, Z. G., Liu, G. X., Yin, Q., and Luo, H. Y. (2016). Characteristics of shale pores, fractal dimension and their controlling factors determined by nitrogen adsorption and mercury injection methods. *Petrol. Geol. Rec. Eff.* 23 (2), 1–8. doi:10.13673/j.cnki.cn37-1359/te.20151215.002

Cheng, Y., Liu, C., Wu, W., Wen, M. Y., Nie, Q., and Lu, P. (2018). The application of argon ion polishing-environmental scanning electron microscopy to the research on shale nanometer-sized pores-Taking Sha-1 member in JX area as an example. *J. Chin. Electron Microsc. Soc.* 37 (1), 52–58. doi:10.3969/j.issn.1000-6281.2018.01.008

Dou, J. N., Lin, Y. Q., Shao, F., and Dong, H. M. (2020). Advances in characterization techniques and experimental methods of shale gas reservoir pore structure. *J. Xi'an Univ. Sci. Tech.* 40 (6), 1019–1030. doi:10.13800/j.cnki.xakjdxxb.2020.0612

Fan, C. H., Li, H., Qin, Q. R., He, S., and Zhong, C. (2020a). Geological conditions and exploration potential of shale gas reservoir in Wufeng and Longmaxi Formation of southeastern Sichuan Basin, China. *J. Petrol. Sci. Eng.* 191, 107138. doi:10.1016/j.petrol.2020.107138

Fan, C. H., Li, H., Zhao, S. X., Qin, Q. R., Fan, Y., Wu, J. F., et al. (2020b). Formation stages and evolution patterns of structural fractures in marine shale: case study of the Lower Silurian Longmaxi Formation in the Changning area of the southern Sichuan Basin, China. *Energy Fuel* 34 (8), 9524–9539. doi:10.1021/acs.energyfuels.0c01748

Fan, C. H., Nie, S., Li, H., Radwan, A. E., Pan, Q. C., Shi, X. C., et al. (2024). Quantitative prediction and spatial analysis of structural fractures in deep shale gas reservoirs within complex structural zones: a case study of the Longmaxi Formation in the Luzhou area, southern Sichuan Basin, China. *J. Asian Earth Sci.* 263, 106025. doi:10.1016/j.jseaes.2024.106025

Gao, Z., Fan, Y., Xuan, Q., and Zheng, G. (2020). A review of shale pore structure evolution characteristics with increasing thermal maturities. *Adv. Geo-Energy Res.* 4 (3), 247–259. doi:10.46690/ager.2020.03.03

Hao, M. Z., Jiang, Z. X., Nie, Z., Xue, Z. X., Zhong, G. H., He, S. J., et al. (2022). Development characteristics of pore connectivity in deep shale reservoirs and its controlling factors:a case study of Longmaxi Formation in southern Sichuan Basin. *Fault-Block Oil Gas. Field* 29 (6), 761–768. doi:10.6056/dkyqt202206007

He, S., Qin, Q. R., Li, H., and Wang, S. L. (2022b). Deformation differences in complex structural areas in the southern sichuan basin and its influence on shale gas preservation: a case study of changning and luzhou areas. *Front. Earth Sci.* 9, 818534. doi:10.3389/feart.2021.818534

He, S., Qin, Q. R., Li, H., and Zhao, S. X. (2022a). Geological characteristics of deep shale gas in the silurian Longmaxi Formation in the southern sichuan basin, China. *Front. Earth Sci.* 9, 818543. doi:10.3389/feart.2021.818155

Huang, Y. Q., Zhang, P., Zhang, J. C., and Yang, J. W. (2020). The Effect on the fractal characteristics of shale pores by mineral compositions of marine and marine-continental transitional shales. *Bull. Mineral. Petrol. Geoch.* 39 (3), 548–557. doi:10.19658/j.issn.1007-2802.2020.39.026

Jiang, Z. X., Tang, X. L., Li, Z., Huang, H. X., Yang, P. P., Yang, X., et al. (2016). The whole-aperture pore structure characteristics and its effect on gas content of the Longmaxi Formation shale in the southeastern Sichuan basin. *Earth Sci. Front.* 23 (2), 126–134. doi:10.13745/j.esf.2016.02.013

Kong, X. X., Xiao, D. S., Jiang, S., Lu, S. F., Sun, B., and Wang, J. M. (2020). Application of the combination of high-pressure mercury injection and nuclear magnetic resonance to the classification and evaluation of tight sandstone reservoirs: a case study of the Linxing Block in the Ordos Basin. *Nat. Gas. Ind.* 40 (3), 38–47. doi:10.3787/j.issn.1000-0976.2020.03.005

Li, B., Chen, F. W., Xiao, D. S., Lu, S. F., Zhang, L. C., Zhang, Y. Y., et al. (2019b). Effect of particle size on the experiment of low temperature nitrogen adsorption: a case study of marine gas shale in Wufeng-Longmaxi formation. *J. China Univ. Min. Tech.* 48 (2), 395–404. doi:10.13247/j.cnki.jcumt.000931

Li, H. (2023). Coordinated development of shale gas benefit exploitation and ecological environmental conservation in China: a mini review. *Front. Ecol. Evol.* 11, 1232395. doi:10.3389/fevo.2023.1232395

Li, H., Tang, H. M., Qin, Q. R., Wang, Q., and Zhong, C. (2019c). Effectiveness evaluation of natural fractures in Xujiahe Formation of Yuanba area, Sichuan basin, China. *Arab. J. Geosci.* 12 (6), 194. doi:10.1007/s12517-019-4292-5

Li, H., Tang, H. M., and Zheng, M. J. (2019a). Micropore structural heterogeneity of siliceous shale reservoir of the Longmaxi Formation in the southern Sichuan Basin, China. *Minerals* 9, 548. doi:10.3390/min9090548

Li, J. J., Qin, Q. R., Li, H., and Wan, Y. F. (2022). Numerical simulation of the stress field and fault sealing of complex fault combinations in Changning area, Southern Sichuan Basin, China. *Energy Sci. Eng.* 10 (2), 278–291. doi:10.1002/ese3.1044

Li, K., Kong, S., Xia, P., and Wang, X. (2020). Microstructural characterisation of organic matter pores in coal-measure shale. *Adv. Geo-Energy Res.* 4 (4), 372–391. doi:10.46690/ager.2020.04.04

Li, Y. Z. (2021). Mechanics and fracturing techniques of deep shale from the Sichuan Basin, SW China. *Energy Geosci.* 2 (1), 1–9. doi:10.1016/j.engeos.2020.06.002

Liu, K., and Ostadhassan, M. (2019). The impact of pore size distribution data presentation format on pore structure interpretation of shales. *Adv. Geo-Energy Res.* 3 (2), 187–197. doi:10.26804/ager.2019.02.08

Liu, R. B., Wei, Z. H., Jia, A. Q., He, S., Hou, Y. G., He, Q., et al. (2023). Fractal Characteristics of pore structure in deep overpressured organic-rich shale in Wufeng-Longmaxi Formation in Southeast Sichuan and its geological significance. *Earth Sci.* 48 (4), 1496–1516. doi:10.3799/dqkx.2022.177

Luo, S. Y., Chen, X. H., Liu, A., Li, H., and Sun, C. (2019a). Characteristics and geological significance of canister desorption gas from the Lower Cambrian Shuijingtuo Formation shale in Yichang area, Middle Yangtze region. *Acta Pet. Sin.* 40 (8), 941–955. doi:10.7623/syxb201908005

Luo, S. Y., Chen, X. H., Liu, H., Liu, A., and Wang, S. C. (2019b). Shale gas accumulation conditions and target optimization of lower cambrian Shuijingtuo Formation in Yichang area, west Hubei. *Earth Sci.* 44 (11), 3598–3615. doi:10.3799/dqkx.2019.179

Ma, R. Y., Zhang, J., Wang, M., Ma, W. P., and Zhao, J. G. (2021). Micro-pore characteristics and gas-bearing properties of marine continental transitional shale reservoirs in the Qinshui basin. *J. Henan Polytech. Univ.* 40 (4), 66–77. doi:10.16186/j.cnki.1673-9787.2019120015

Shi, D. S., Xu, Q. C., Guo, R. L., Liu, E. R., Zhu, D. S., Wang, H., et al. (2023). Pore structure characteristics and main controlling factors of Permian organic-rich shale in Lower Yangtze Region. *Nat. Gas. Geosci.* 33 (12), 1911–1925. doi:10.11764/j.issn.1672-1926.2022.09.005

Sun, Z. L., Wang, F. R., Han, Y. J., Hou, Y. G., He, S., Zheng, Y. H., et al. (2021). Characterization and evaluation of fractal dimension of intersalt shale oil reservoirs in Qianjiang Depression. *Bull Geol. Sci. Tech.* 41 (4), 125–137. doi:10.19509/j.cnki.dzkq.2021.0063

Tian, H., Zhang, S. C., Liu, S. B., Wang, M. Z., Zhang, H., Hao, J. Q., et al. (2016). The dual influence of shale composition and pore size on adsorption gas storage mechanism of organic-rich shale. *Nat. Gas. Geosci.* 27 (3), 494–502. doi:10.11764/j.issn.1672-1926.2016.03.0494

Wang, K. L., Li, K. Q., Wang, L. K., Gao, H. L., Wang, K. W., and Hu, P. Q. (2018). Mineral composition and gas-bearing characteristics of Wufeng-Longmaxi shale in Shizhu area, eastern Sichuan Basin. *J. Lanzhou Univ.* 54 (3), 285–291. doi:10.13885/j.issn.0455-2059.2018.03.001

Wang, X., Qi, M., Hu, Y. L., and Qiu, Y. S. (2015). Analysis of the shale pore structures by the combination of high-pressure mercury injection and fractal theory. *Petrol. Geol. Oilfield Dev. Daqing* 34 (2), 165–169. doi:10.3969./J.ISSN.1000-3754.2015.02.033

Wu, Y. H., and Lei, T. Z. (2022). Influence of hydrogenation at different temperatures on hydrocarbongeneration of source rocks. *J. Chongqing Univ.* 45 (5), 43–51. doi:10.11835/j.issn.1000-582x.2022.05.005

Xia, D. L., Wu, Y., Zou, M., Xia, D. D., and Pang, W. (2022). Quality characterization of tight sandstone reservoirs in the yanchang formation of the honghe oilfield, ordos basin, central China. *Energy Geosci.* 3 (4), 444–452. doi:10.1016/j.engeos.2021.07.001

Xie, W. D., Wang, M., Wang, H., and Duan, Q. Y. (2022). Multi-scale fractal characteristics of pores in transitional shale gas reservoir. *Nat. Gas. Geosci.* 33 (3), 451–460. doi:10.11764/j.issn.1672-1926.2021.06.006

Xiong, J., Liu, X. J., Liang, L. X., and Zeng, Q. (2017). Adsorption of methane in organic-rich shale nanopores: an experimental and molecular simulation study. *Fuel* 200, 299–315. doi:10.1016/j.fuel.2017.03.083

Xu, L. L., Wen, Y. R., Zhou, X. H., Ju, Z. L., Chen, H., Yang, J., et al. (2022). Paleo-environment of the first member of Niutitang Formation on the southern margin of Huangling anticline, western Hubei province:a case study of well ZD-1. *Petroleum Geol. Exp.* 44 (3), 456–465. doi:10.11781/sysydz202203456

Yin, S. L., Xie, J. Y., Cheng, L. L., Wu, Y. X., Zhu, B. Y., Chen, G. Y., et al. (2022). Advances in continental shale oil research and problems of reservoir geology. *Acta Sedimentol. Sin.* 40 (4), 979–995. doi:10.14027/j.issn.1000-0550.2021.109

Zeng, H. B., Wang, F. R., Luo, J., Tao, T., and Wu, S. Q. (2021). Characteristics of pore structure of intersalt shale oil reservoir by low temperature nitrogen adsorption and high pressure mercury pressure methods in Qianjiang Sag. *Bull. Geol. Sci. Tech.* 40 (5), 242–252. doi:10.19509/j.cnki.dzkq.2021.0022

Zhang, J. Z., Zhu, D., Ci, X. H., Niu, Q., Zhang, H. X., Tang, Y. C., et al. (2019). Characteristics of carbon isotope while drilling and exploration significance of shale gas in Niutitang and Doushantuo formations in Well Eyangye-2,Yichang, Hubei, China. Acta Petrol. *Sin.* 40 (11), 1346–1357. doi:10.7623/syxb201911005

Zhang, L. L., Chen, G. X., Le, X. F., Zhang, Y., Shao, D. Y., Yan, J. P., et al. (2023a). Significance of water absorption characteristics and difference of pore structures in the Cambrian shale intervals, Yichang area for shale reservoir evaluation. *Earth Sci. Front.* 30 (3), 138–150. doi:10.13745/j.esf.sf.2022.5.38

Zhang, Q., Liang, F., Liang, P. P., Zhou, S. W., Guo, W., Guo, W., et al. (2020). Investigation of fractal charactrtistics and its main controlling factors of shale reservoir: a case study of the Longmaxi shale in Weiyuan shale gas field. *J. China Univ. Min. Techn.* 49 (1), 110–122. doi:10.13247/j.cnki.jcumt.001068

Zhang, Y., Huang, D., Zhang, L. L., Wan, C. H., Luo, H., Shao, D. Y., et al. (2023b). Biogenic silica of the lower cambrian Shuijingtuo Formation in Yichang,western Hubei province-features and influence on shale gas accumulation. *Earth Sci. Front.* 30 (3), 83–100. doi:10.13745/j.esf.sf.2022.5.40

Zhao, J. L., Tang, D. Z., Xu, H., and Xu, H. (2015). Fine characterization of the shale micropore structures based on the carbon dinxide adsorption experiment. Petrol. *Geol. Oilfield Dev. Daqing.* 34 (5), 156–161. doi:10.3969/J.ISSN.1000-3754.2015.05.030

Zhao, Y., Li, L., Si, Y. H., and Wang, H. M. (2022). Fractal characteristics and controlling factors of pores in shallow shale gas reservoirs: a case study of Longmaxi Formation in Zhaotong area, Yunnan Province. *J. Jilin Univ.* 52 (6), 1813–1829. doi:10.13278/j.cnki.jjuese.20220148

Zhu, W. C., Niu, L. L., and Li, S. H. (2019). Creep-impact test of rock: Status-of-the-art and prospect. *J. Min Strata Control Eng.* 1 (1), 013003. doi:10.13532/j.jmsce.cn10-1638/td.2019.02.007

Zuo, J. P., Yu, M. L., and Hu, S. Y. (2019). Experimental investigation on fracture mode of different thick rock strata. *J. Min Strata Control Eng.* 1 (1), 013007. doi:10.13532/j.jmsce.cn10-1638/td.2019.02.008